JMEPEG (2010) 19:1337–1343
DOI: 10.1007/s11665-010-9627-z

1059-9495/$19.00

Deformation Behavior and Constitutive Equation Coupled the Grain Size of Semi-Solid Aluminum Alloy

Yalin Lu, Miaoquan Li, and Xingcheng Li

(Submitted September 14, 2009; in revised form January 14, 2010)

Isothermal compression tests on Al-4Cu-Mg alloy were carried out in semi-solid state. Deformation behavior and microstructural evolution are discussed in this paper. Meanwhile, a new constitutive equation, which couples the grain size and liquid volume fraction, has been established for the semi-solid deformation behavior. The results show that the maximum difference between the calculated with the experimental data is less than 15%. The present equation is satisfactory for describing the correlation between the flow stress and microstructure of semi-solid Al-4Cu-Mg alloy. The coupled simulation of the deformation behavior and microstructural evolution during the semi-solid forming would be conducted easily through writing the present equation in a FE code.

Keywords constitutive equation, deformation behavior, microstructural evolution, semi-solid state

1. Introduction

With the wide application of finite element modeling in semi-solid forming, it is essential to establish a reasonable mathematical description on the flow stress curves so as to improve the accuracy of finite element simulation. In the past several decades, much work has been done in the field (Ref 1-11). Joly et al. (Ref 1) proposed an experimental formulation to describe the relation between flow stress, strain rate and solid fraction. Haaften et al. (Ref 2) constructed a mathematical description to illuminate the tension behavior of semi-solid AA3104 and AA5182 based on Arrhenius equation. Gunasekera et al. (Ref 3) defined the relationship between the flow stress and strain as a function of liquid fraction and a shape factor using the geometric shape of the solid particle. During the semi-solid compression of A356 alloy, Kang et al. (Ref 4) found that the flow stress increases with an increase of strain at initial stage of deformation. Above peak stress, the flow stress decreases gradually with an increase of strain. When strain reaches a critical value, the flow stress increases sequentially. Meanwhile, macroscopic phase segregation occurred with densification of the remaining solid in the central region. Based on analyzing Gunasekera' research and experimental results, Kang et al. (Ref 4) put forward a viscoplastic model, in which geometric factor and separation coefficient are introduced. Ding et al. (Ref 5) constructed rigid viscoplastic constitutive model according to analysis on the flow stress of AlSi7Mg alloy during the semi-solid compression.

The flow stress of semi-solid alloy is affected by process parameters, such as strain, strain rate, deformation temperature, etc., and can be represented as a function of macroparameters at present. However, it is known that deformation behavior is also influenced by microstructure evolution during semi-solid deformation. In this paper, a constitutive equation is proposed based on the effects of microstructural evolution during semi-solid deformation. The present equation has been applied to describe a correlation of the flow stress with the microstructure evolution of the Al-4Cu-Mg alloy in semi-solid state.

2. Experimental Procedures

The experimental material, which was fabricated by a strain induced melt activation process (SIMA) (Ref 12), was the semi-solid Al-4Cu-Mg alloy with near-equiaxed grains, which the solidus and liquidus of this alloy are 504.9 and 643.3 °C, respectively.

Cylindrical specimens 8 mm in diameter and 12 mm in height were compressed in a THERMECMASTOR-Z simulator. The specimens and compression rams were heated by a high-frequency induction-heating system under vacuum conditions to avoid oxidation. The lower ram was fixed and the upper ram was moved up and down on the crosshead to given strain rates. Chromel-alumel thermo-couples, which were welded at the middle of the specimens, were used to measure and monitor the specimen temperature during the compression. The specimens were held 3 min to equilibrate the temperature field of the whole specimen and melt adequately the low melting point phase at the given deformation temperature prior to deformation. Subsequently, the specimens were immediately cooled by nitrogen gas at a rate of 30 K s^{-1} after compression to retain the as-deformed microstructures.

In this work, specimens were compressed to height reductions (e) of 20, 40 and 60% at strain rates ($\dot{\varepsilon}$) of 0.001, 0.01, 0.1 and 1 s^{-1}. The deformation temperatures (T) were 540, 560 and 580 °C at each combination of strain rate and height

Yalin Lu, School of Materials Science and Engineering, Northwestern Polytechnical University, Xi'an, China and School of Mechanical Engineering, Jiangsu Teachers University of Technology, Changzhou, China; **Miaoquan Li**, School of Materials Science and Engineering, Northwestern Polytechnical University, Xi'an, China; and **Xingcheng Li**, School of Mechanical Engineering, Jiangsu Teachers University of Technology, Changzhou, China. Contact e-mails: honeymli@nwpu.edu.cn and luyalin@163.com

reduction. The microstructural observations and measurements of microstructural variables, including grain size, solid volume fraction, were carried out using an OLYMPUS PMG3 microscope for quantitative metallography linked to a SISC IAS V8.0 analysis software. At the cross-section of the specimens, five fields are chosen and microstructural variables are measured at four points around a field. Finally, the average value about 20 points is the measurement result of microstructural variables.

3. Experimental Results and Discussion

3.1 Flow Stress

Typically true stress-strain curves of semi-solid Al-4Cu-Mg alloy obtained at different process parameters are shown in Fig. 1. The flow stress at deformation temperatures of 540 and 560 °C reaches a peak value at a true strain of 0.02. Then, the flow stress drops markedly with true strain and reaches a steady value at a true strain of 0.05. The larger the deformation temperature is, the lower the flow stress is during the semi-solid deformation. From Fig. 1(a)-(d), true stress-strain curves at deformation temperatures of 540 and 560 °C are different from those at a deformation temperature of 580 °C. The flow stress varies slightly with true strain because of the high volume fraction of the liquid phase at a deformation temperature of 580 °C. Therefore, a high deformation temperature should be chosen in order to decrease the load. From Fig. 1, there is an optimal value of the deformation temperature from 560 to 580 °C.

From Fig. 1, the flow stress is influenced by strain rates at same deformation temperature. The flow stress decreases markedly with a decrease of strain rate. At a low strain rate, there is more time for the liquid phase to distribute uniformly at the grain boundaries, which results in the easy movement of the solid phase and a decrease of the flow stress.

3.2 Microstructure Evolution

Figure 2 illustrated the microstructure of Al-4Cu-Mg alloy during semi-solid compression at different deformation temperature. From Fig. 2, morphology of α solid particle varies significantly with the deformation temperatures. Due to low deformation temperature of 540 °C, the liquid phase is so less that it cannot soak into the grain boundaries. So, the grain boundaries are not clear and discontinuous as shown in Fig. 2(a). At the deformation temperature of 560 °C, α grains are separated from each other because of liquid phase soakage between the grain boundaries as shown in Fig. 2(b). When the deformation temperature is up to 580 °C, α grains coarsen gradually and become more globular as shown in Fig. 2(c).

From Fig. 2, liquid phase fraction at different deformation temperature is related to deformation mechanism during semi-solid compression. It is observed that, when deformation temperature is low, liquid phase is less accordingly. Due to low liquid fraction at the low deformation temperature, PDS (plastic deformation of solid particles) is a dominating mechanism. With an increase of deformation temperature, the major mechanisms transform gradually from PDS (plastic deformation

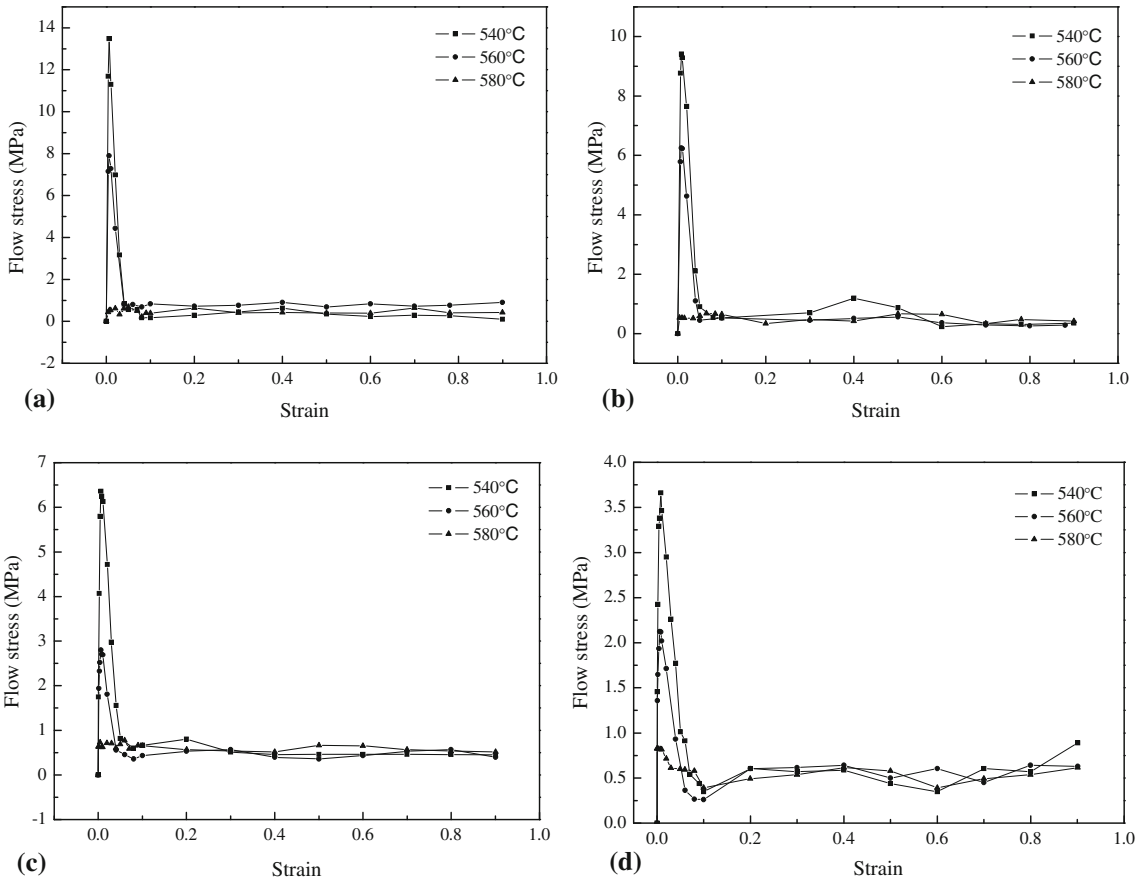

Fig. 1 Stress-strain curves during the semi-solid compression of Al-4Cu-Mg alloy. (a) 1 s^{-1}; (b) 0.1 s^{-1}; (c) 0.01 s^{-1}; (d) 0.001 s^{-1}

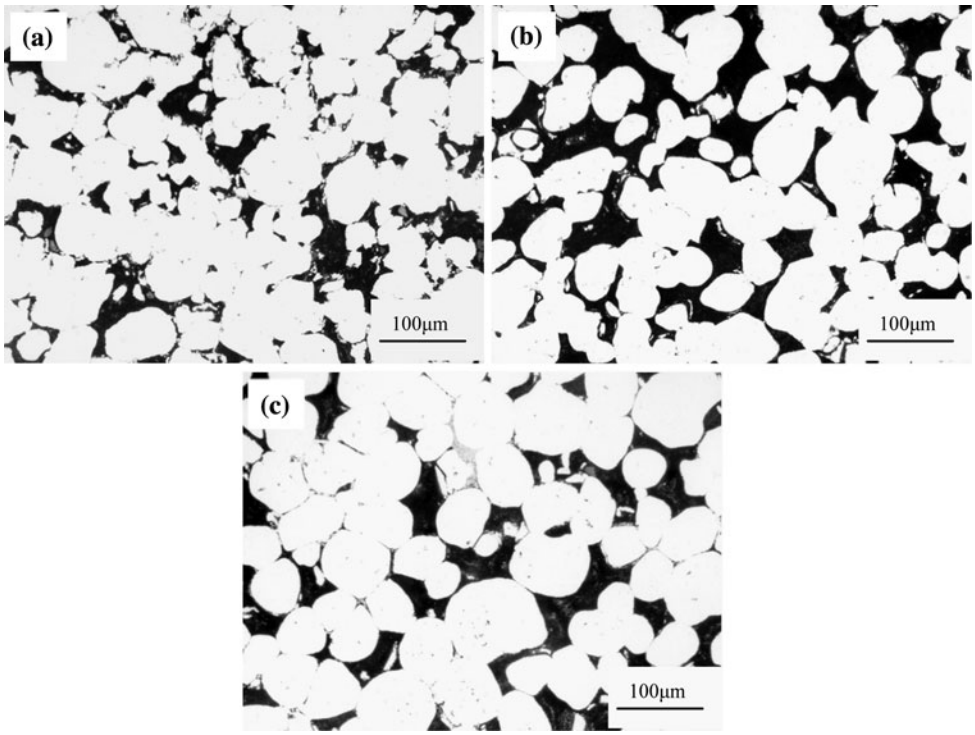

Fig. 2 Microstructures of semi-solid Al-4Cu-Mg alloy at different deformation temperatures. (a) 540 °C; (b) 560 °C; (c) 580 °C

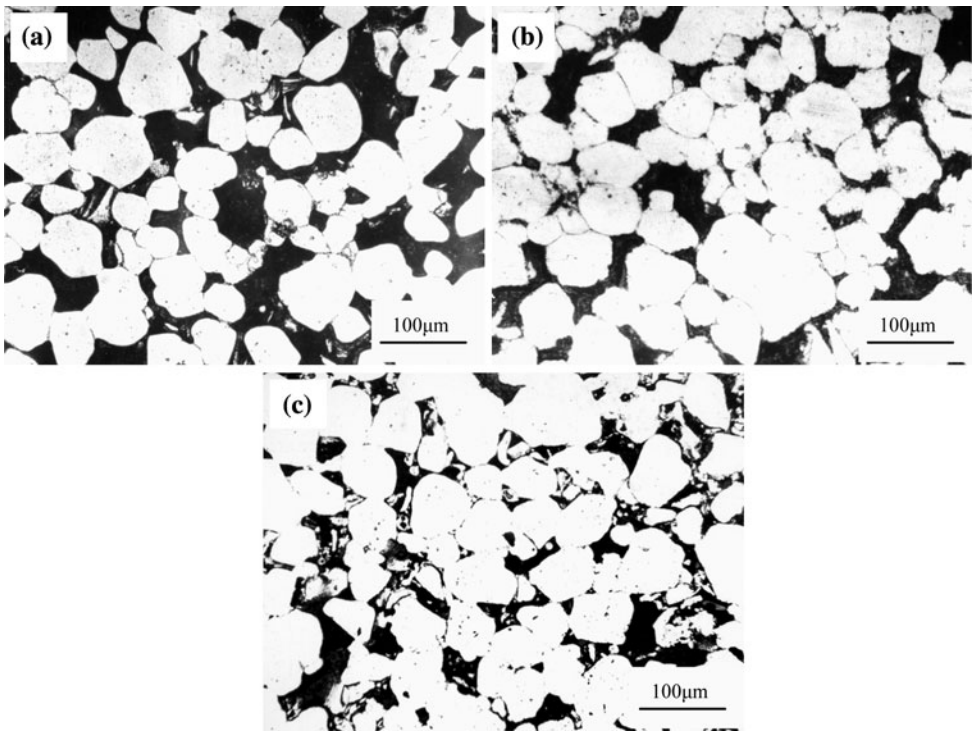

Fig. 3 Microstructures of semi-solid Al-4Cu-Mg alloy at different strains. (a) 20%; (b) 40%; (c) 60%

of solid particles) to SS (sliding between the solid particles) and FLS (flow of liquid incorporating solid particles), which are promoted coarsening of α grains.

The effects of height reduction on the microstructures are shown in Fig. 3. Morphology of α grain is more globular at low height reduction than that at high height reduction. The reason is that liquid phase is extruded from the center to the free surface. The greater the height reduction, the more plastic deformation between solid particles occurs at the large deformation region.

Figure 4 shows microstructures of semi-solid Al-4Cu-Mg alloy at different strain rates. From Fig. 4, α grains gradually

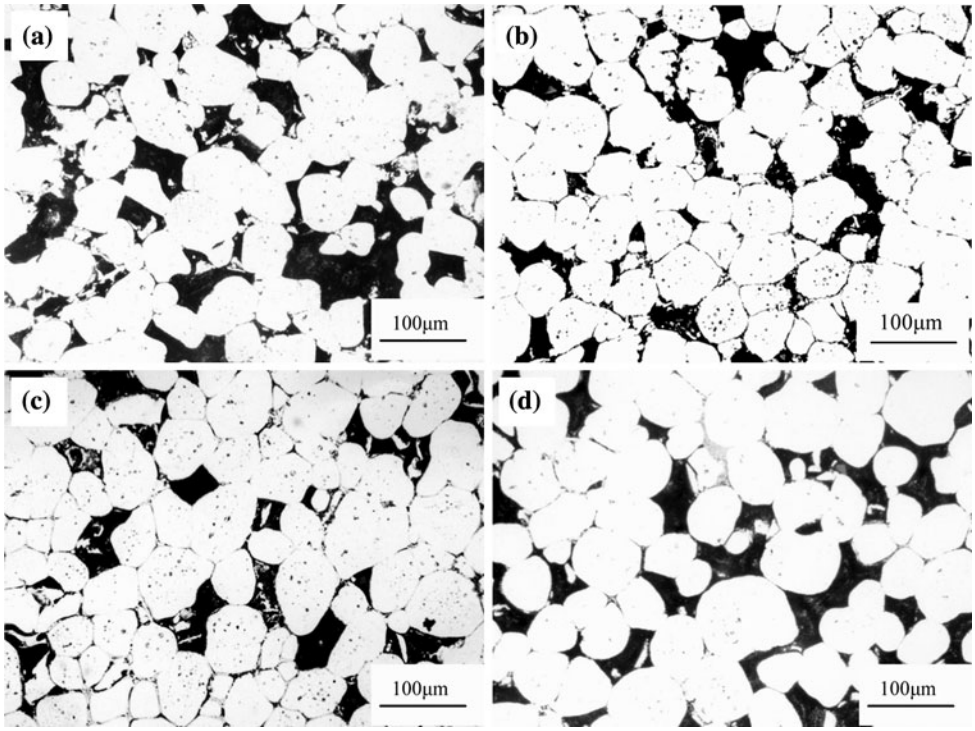

Fig. 4 Microstructure of semi-solid Al-4Cu-Mg alloy at different strain rates. (a) 1 s^{-1}; (b) 0.1 s^{-1}; (c) 0.01 s^{-1}; (d) 0.001 s^{-1}

coarsen and become more globular with a decrease of the strain rate. At low strain rate of 0.01-0.001 s^{-1}, α grains adjoining each other coalesce and coarsen gradually as shown in Fig. 4(c) and (d). So, there is more time for the solid particles to coarsen and become globular when strain rate is low.

The effects of the process parameters on grain size of the semi-solid Al-4Cu-Mg alloy are shown in Fig. 5. From Fig. 5(a), the effect of height reduction on grain size depends on deformation temperature. When deformation temperature is less than 580 °C, size of α grains decreases with an increase of height reduction. Above deformation temperature of 580 °C, size of α grains increases with an increase of height reduction. The effect of deformation temperature on grain size is shown in Fig. 5(b). In general, size of α grains increases with an increase of the deformation temperature, which results from coalescence and coarsening occurred between the adjoining grains with an increase of the deformation temperature. The effect of strain rate on grain size of the semi-solid Al-4Cu-Mg alloy is shown in Fig. 5(c). Size of grain decreases with an increase of strain rate when strain rate is less than 0.1 s^{-1}. Size of grain increases with an increase of strain rate when strain rate is above 0.1 s^{-1}. The reason might be attributed to different deformation mechanisms.

4. Constitutive Equation Coupled Microstructural Variables

4.1 Establish of Constitutive Equation

Based on analysis the experimental results of semi-solid Al-4Cu-Mg alloy, the flow stress is influenced both the deformation process parameters and microstructural evolution. So, the dependence of flow stress on the deformation process parameters and microstructural variables in semi-solid state is expressed in term of an equation given by

$$\sigma = F_1 \cdot F_2 \qquad \text{(Eq 1)}$$

where σ is the flow stress of materials (MPa), F_1 is a function of the process parameters on the flow stress, F_2 is a function of microstructural evolution during the semi-solid deformation, which presented the whole influence of microstructural evolution from begin to current stage on the flow stress.

In Eq 1, F_1 depends on the deformation temperature, strain rate, strain and liquid volume fraction, and is described in Eq 2:

$$F_1\colon \sigma = \dot{\varepsilon}^m \varepsilon^n \exp(a - bT)(1 - \beta f_l)^k \qquad \text{(Eq 2)}$$

where σ is flow stress of materials (MPa), $\dot{\varepsilon}$ is the strain rate (s^{-1}), ε is strain, T is the absolute deformation temperature (K), f_l is the liquid volume fraction at current stage, which can be calculated through a model of artificial neural networks (Ref 13), β is a constant considering the geometric shape, and β value is generally 1.428 (Ref 4), *m, n, a, b* and *k* are material constants.

During the semi-solid deformation, microstructural evolution influences directly the deformation behavior. So, a function F_2 is described in Eq 3 based on effect of microstructural evolution on deformation behavior.

$$F_2\colon f(d) = A_0 + A_1(d/d_0) + A_2(d/d_0)^2 \qquad \text{(Eq 3)}$$

where d_0 is the average grain size at beginning of deformation (μm), d is the average grain size at semi-solid

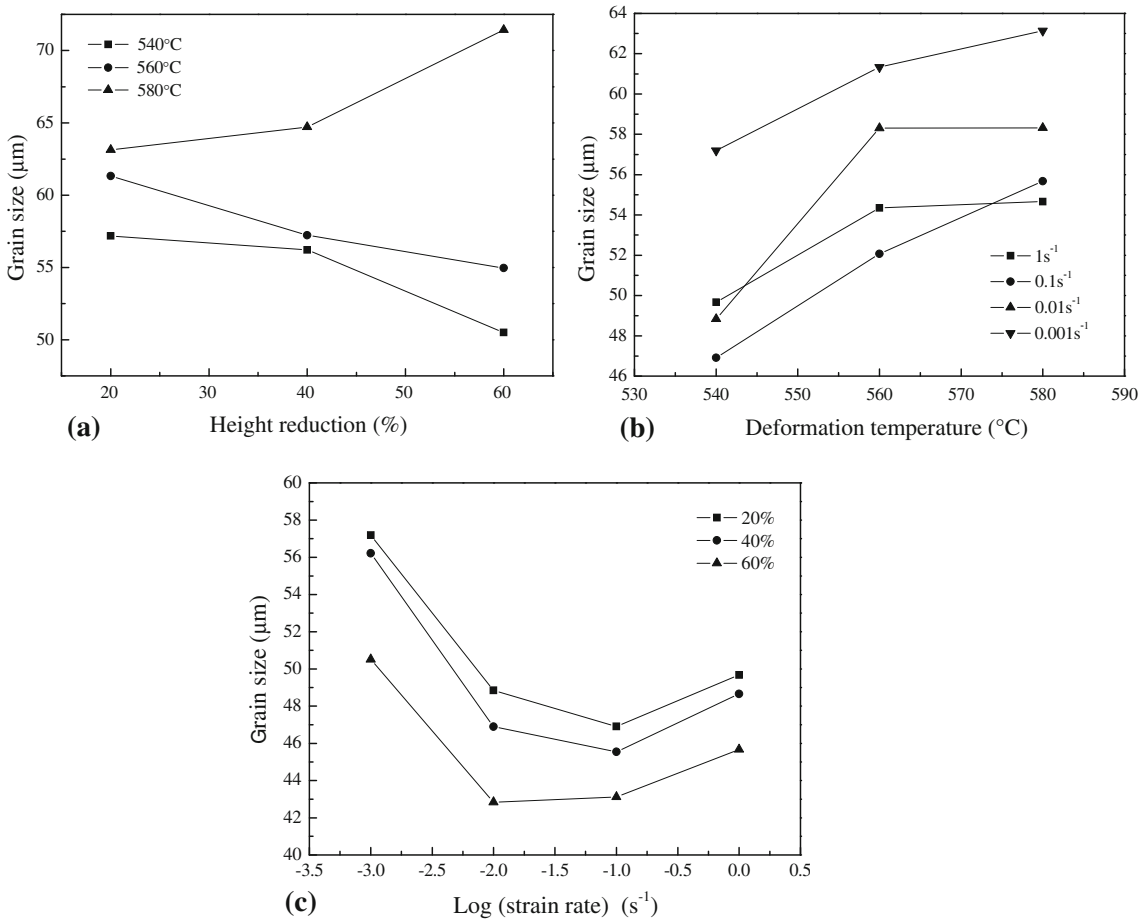

Fig. 5 Effects of the process parameters on grain size of the semi-solid Al-4Cu-Mg alloy. (a) Height reduction; (b) deformation temperature; (c) strain rate

Table 1 Deformation activation energy Q at different strain rates

$\dot{\varepsilon}$, s^{-1}	1	0.1	0.01	0.001
Q, kJ/mol	241.15	229.73	173.36	143.94

deformation temperature (μm), which can be calculated through the model of artificial neural networks (Ref 13). A_0, A_1 and A_2 is a function of ln Z respectively, and calculated in Eq 4. x is defined as ln Z, and Z is the Zener-Hollomon parameter $[\dot{\varepsilon}\exp(Q/RT)]$.

$$f_1(x) = B_0 + B_1x + B_2x^2 + B_3x^3 \quad \text{(Eq 4)}$$

where B_0, B_1, B_2 and B_3 are material constants. $\dot{\varepsilon}$ is the strain rate (s^{-1}), Q is the activation energy of deformation (kJ/mol) and the values are shown in Table 1, T is the absolute deformation temperature (K), and R is the gas constant (kJ/mol · K^{-1}).

4.2 Determining of Materials Constants

Based on the experimental results for the Al-4Cu-Mg alloy, the constants in the present equation were obtained by the least square method. The constants in Eq 2 are shown in Table 2 and the constants in Eq 3 and 4 are shown in Table 3.

Table 2 The constants of the Al-4Cu-Mg alloy (part 1)

Constants	m	n	a	b	k
Results	0.06912	−0.46724	11.0245	0.01489	1.80806

Table 3 The constants of the Al-4Cu-Mg alloy (part 2)

Constants	B_0	B_1	B_2	B_3
A_0	424.96911	−54.03524	2.12040	−0.02796
A_1	−973.32707	124.93101	−4.96547	0.06619
A_2	560.66288	−72.40457	2.91109	−0.03916

4.3 Verification of the Constitutive Equation

Figure 6 shows the comparison between the calculated results for the Al-4Cu-Mg alloy using the present constitutive equation and experimental results. The maximum difference between the calculated and experimental results is less than 15%.

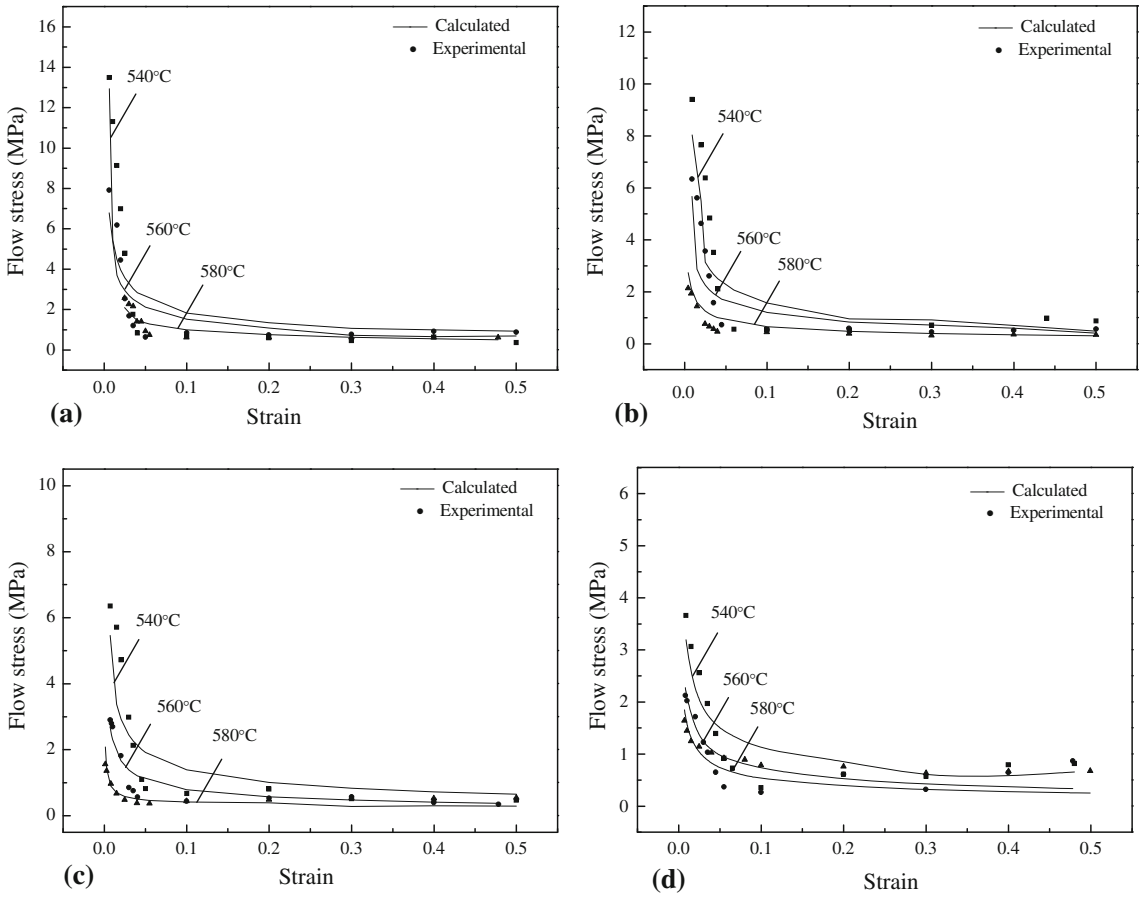

Fig. 6 Comparison of the calculated with the experimental results of flow stress. (a) 1 s^{-1}; (b) 0.1 s^{-1}; (c) 0.01 s^{-1}; (d) 0.001 s^{-1}

5. Conclusions

During semi-solid forming of Al-4Cu-Mg alloy, deformation behavior and microstructure are affected significantly by the process parameters, including deformation temperature, height reduction and strain rate. Based on the experimental results from the semi-solid Al-4Cu-Mg alloy, a constitutive equation coupled microstructural variables has been established considering the change in grain size and liquid volume fraction in this paper. The present equation is satisfactory for describing the correlation between the flow stress and microstructure evolution of semi-solid Al-4Cu-Mg alloy. Comparison of the calculated with the experimental results, the maximum difference is less than 15%. The present equation would be easy to write in a FE code, so as to simulate the change in grain size and liquid volume fraction during the semi-solid forming. Therefore, the coupled simulation of the deformation behavior with microstructure could be carried out.

Acknowledgment

This research has been supported by the Foundational Research Plan of Jiangsu Province (No. BK2005025).

References

1. P.A. Joly and R. Mehrabian, The Rheology of a Partially Solid Alloy, *J. Mater. Sci.*, 1976, **11**, p 1393–1418
2. W.M. Van Haaften, W.H. Kool, and L. Katerman, Tensile Behavior of Semisolid Industrial Aluminum Alloys AA3104 and AA5182, *Mater. Sci. Eng. A*, 2002, **336**, p 1–6
3. J.S. Gunasekera, Development of a Constitutive Model for Mushy Materials, *Proceedings of the 2nd International Conference on Semi-Soild Processing of Alloys and Composites*, Cambridge, USA, 1992, p 211–222
4. C.G. Kang and H.K. Jung, Finite Element Analysis with Deformation Behavior Modeling of Globular Microstructure in Forming Process of Semi-Solid Materials, *Int. J. Mech. Sci.*, 1999, **41**, p 1423–1445
5. R. Kopp, J. Choi, and D. Neudenberger, Simple Compression Test and Simulation of an Sn-15%Pb Alloy in the Semi-Solid State, *J. Mater. Process. Technol.*, 2002, **6376**, p 1–7
6. J.H. Yoon, Y.T. Im, and N.S. Kim, Finite Element Modeling of the Deformation Behavior of Semi-Solid Materials, *J. Mater. Process. Technol.*, 2001, **113**, p 153–159
7. A. Rassili, C. Geuzaine, and W. Legros, Numerical Simulations and Experimental Investigations of the Semi-Solid Metal Processing of Steels, *Proceedings of the 7th International Conference on Semi-Solid Processing of Alloys and Composites*, Tsukuba, Japan, 2002, p 367–372
8. X.G. Li, S.S. Xie, and Y.X. Jiang, Rigid-Viscoplastic Finite Element Analysis on Semi-Solid Thixoforming Automobile Wheel of AZ91D Magnesium Alloy, *Proceedings of the 8th International Conference on*

Semi-Solid Processing of Alloys and Composites, Limassol, Cyprus, 2004, p 377–383

9. D. Larouche, J. Langlais, W.L. Wu, and M. Bouchard, A Constitutive Model for the Tensile Deformation of a Binary Aluminum Alloy at High Fractions of Solid, *Metall. Mater. Trans.*, 2006, **37B**, p 431–443
10. H.P. Pan, Z.Y. Ding, Y.S. Dong, and S.S. Xie, Study of the Constitutive Model for Thixoforming of Semi-Solid AlSi7 Mg Alloy, *Acta Metall. Sin.*, 2003, **139**, p 369–374
11. H.V. Atkinson, Modelling the Semisolid Processing of Metallic Alloy, *Prog. Mater. Sci.*, 2005, **50**, p 341–412
12. H.T. Jiang, X.L. Li, A.M. Xiong, and M.Q. Li, Fabrication and Microstructure Evolution of Semi-Solid LY11 Alloy by SIMA, *J. Mater. Eng. Perform.*, 2003, **12**, p 249–253
13. Y.L. Lu, M.Q. Li, and X.C. Li, Experimental Investigation and Modeling of Microstructural Variables of the Al-4Cu-Mg Alloy, *Mater. Sci. Technol.*, 2008, **24**(7), p 815–821